

Comparison of upstream T_e profiles with divertor heat flux and its implications on parallel and perpendicular transport in the SOL of DIII-D H-mode plasmas

M.A. Makowski¹, C.J. Lasnier¹, G.D. Porter¹, A.W. Leonard², J.A. Boedo³,
J.G. Watkins⁴, and D.N. Hill¹

¹*Lawrence Livermore National Laboratory, Livermore, California 94550, USA.*

²*General Atomics, P.O. Box 85608, San Diego, CA 92186-5608, USA.*

³*University of California-San Diego, La Jolla, California 92093, USA.*

⁴*Sandia National Laboratories, Albuquerque, New Mexico, USA*

I. Introduction

On DIII-D we have performed a series of experiments designed to compare the upstream Thomson and midplane probe measurements of T_e with the downstream divertor heat flux width. We find that there is only a weak dependence of the heat flux width on the temperature gradient scale length, in contrast to the strong dependence predicted by simple two-point models [1]. The UEDGE code [2] has also been used to model a number of the discharges and we find that the flows significantly affect the heat flux profiles.

Correlations between the heat flux width and a wide variety of plasma parameters have been made with the result that the only dependence found is on the plasma current, I_p . No dependence was found on, P_{SOL} , P_{inj} , n_e , B_T , the shear and normalized pressure gradient at the 95% flux surface (s_{95} , α_{95}), nor collisionality. Comparing the DIII-D data with other multi-machine scaling relations, we find best agreement with the JET scaling [3].

II. Comparison of Upstream and Midplane T_e Profiles

Upstream Thomson profiles of T_e and n_e measured at the upper outer region of the plasma at a major radius of 1.94 m were mapped to the midplane for comparison with the heat flux profiles. The profiles and heat flux data were “edge localized mode (ELM) synchronized” using a method of conditionally averaging the data falling between ELMs over many ELM cycles. Independent exponential fits to the core- and scrape-off layer (SOL)-side data were made to obtain measurements of the profile gradient scale lengths as shown in Fig. 1. The core-side fits are clearly biased by the pedestal and not used in the subsequent analysis. SOL layer widths inferred from tanh-fits were also analyzed and showed the same trends as the SOL-side fits. To be consistent with other published data SOL-side gradient scale lengths were used in the following analysis.

A database was established by dividing the shot into 200 ms segments and averaging the various plasma parameters and profile data over this period. Additional parameters, such as

shear and normalized pressure gradient, were included in the database in order to perform regression analysis on them.

III. Heat Flux Widths

Divertor temperature profiles were measured with an IRTV camera mounted on the top of the DIII-D vacuum vessel. The heat flux to the target plate was then inferred using the THEODOR [4] code. To arrive at a heat flux width, offset exponentials, $a_0 + a_1 e^{x/\lambda}$, were fit to both the left hand and right hand sides of the profiles. Figure 2 shows a typical outer divertor heat flux profile mapped to the midplane with offset exponentials fit to both sides of the peak. This was necessary as the baseline on the two sides of the profile were, in general, different. With this method an effective Loarte width (ratio of the integral of the heat flux profile to the peak heat flux) [5] could be calculated resulting in,

$$\lambda_q = (\lambda_{\text{left}} + \lambda_{\text{right}}) \frac{R_{\text{div}} B_{\theta}^{\text{div}}}{R_{\text{mp}} B_{\theta}^{\text{mp}}} ,$$

where the factor, $R_{\text{div}} B_{\theta}^{\text{div}} / R_{\text{mp}} B_{\theta}^{\text{mp}}$, accounts for the flux expansion between the target plate and midplane.

The heat flux widths were fit to power scalings of I_p , P_{SOL} , P_{inj} , n_e , B_T , shear and normalized pressure gradient at the 95% flux surface (s_{95} , α_{95}) and collisionality. The only trend found was an inverse dependence on I_p as shown in Fig. 3. A weak dependence on B_T cannot be ruled out, as there were few good points in the data set at low fields ($B_T < 1.5$ T).

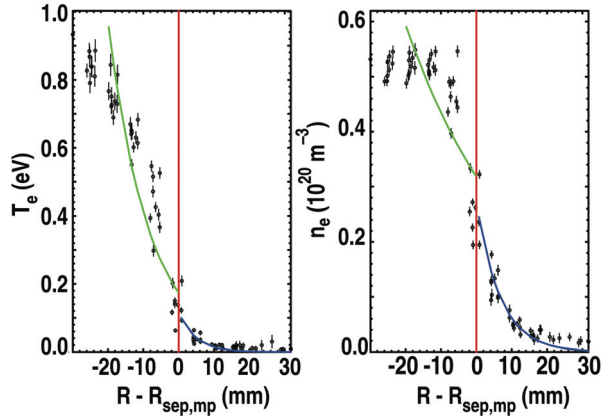


Fig. 1. Upstream profiles of T_e and n_e mapped to the outer midplane. The SOL-side fit was used as a measure of the profile gradient scale length.

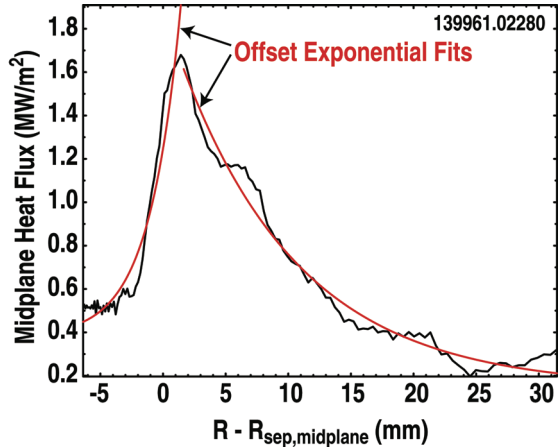


Fig. 2. Typical heat flux profile with offset exponentials fit to each side of the profile.

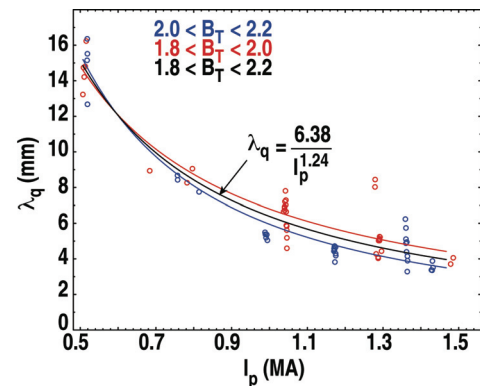


Fig. 3. Plot of the heat flux width, λ_q , versus I_p for two ranges of B_T (red and blue curve fits). Due to the weak dependence of λ_q on B_T , the two curves nearly overlap. The black line is fit to all the data (red and blue circles).

The measured heat flux width, λ_q , shows a very weak dependence on the upstream T_e gradient scale length, λ_{Te} , being essentially uncorrelated. This is shown in Fig. 4, which plots λ_q vs λ_{Te} and the fit to the data. This is in strong disagreement with the simple two-point model [1] that predicts $\lambda_{Te} = (7/2) \lambda_q$. This line is plotted in Fig. 4. Even with the poor correlation, this dependence can be ruled out. The observed weak dependence is not unreasonable as radial transport, SOL radiation, and divertor recycling affect the heat flux within flux tubes; effects not taken into account in the simple model.

IV. Scaling Relations

We have compared our results with several other scaling relations developed for the heat flux width. The first is the JET conduction limited scaling relation [3] given by

$$\lambda_q^{\text{JET}} (\text{mm}) = 2.41 \times 10^{-5} B_T^{-1} (\text{T}) P_{\text{SOL}}^{-1/2} (\text{MW}) n_e^{1/4} (\text{m}^{-3}) q_{95} R^2 (\text{m}) .$$

This is in quite good agreement with our data as shown in Fig. 5, which plots $\lambda_q^{\text{DIII-D}}$ versus λ_q^{JET} . The bulk of the dependence derives from the variation in $q_{95}/B_T \sim 1/I_p$. Our data shows no dependence on n_e , while the JET scaling has a very weak $n_e^{1/4}$ dependence, so there is little variation arising from this term. Our data shows no dependence on P_{SOL} though the JET scaling relation has a $P_{\text{SOL}}^{1/2}$ dependence. Since R is a constant for our data, the remaining scaling relation essentially reduces to $\lambda_q^{\text{JET}} \sim B_T^{-1} q_{95} \sim 1/I_p$. This is quite close to the $I_p^{-1.24}$ scaling found above (Fig. 3).

We have also considered two other multi-machine scaling relations [5]:

$$\lambda_q^{\text{H-1}} (\text{mm}) = 5.2 P_{\text{div}}^{0.44} (\text{MW}) B_T^{-0.45} (\text{T}) q_{95}^{0.57} ,$$

$$\lambda_q^{\text{H-2}} (\text{mm}) = 5.4 P^{0.38} (\text{MW}) B_T^{-0.71} (\text{T}) q_{95}^{0.30} .$$

These are in extremely poor agreement with the DIII-D data. The H-1 scaling predicts a dependence on plasma current of approximately $I_p^{1/2}$ and no size dependence. The H-2 scaling predicts profile

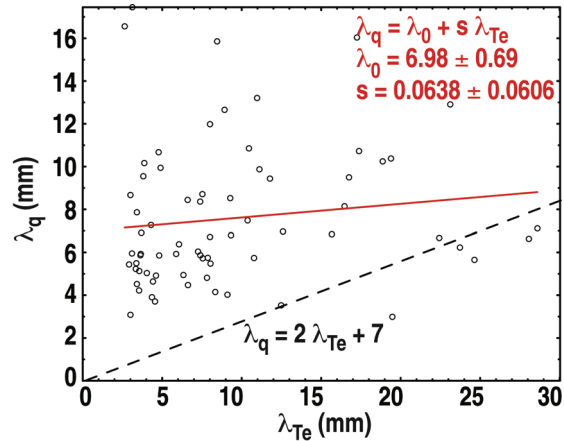


Fig. 4. Plot of the heat flux width, λ_q , vs the Thomson electron profile gradient scale length in the scrape-off layer, $\lambda_{Te,SOL}$. Solid red line is a linear fit between the two parameters. The slope, s , is 1/10th that predicted by simple two-point models. Correlation coefficient = 0.124.

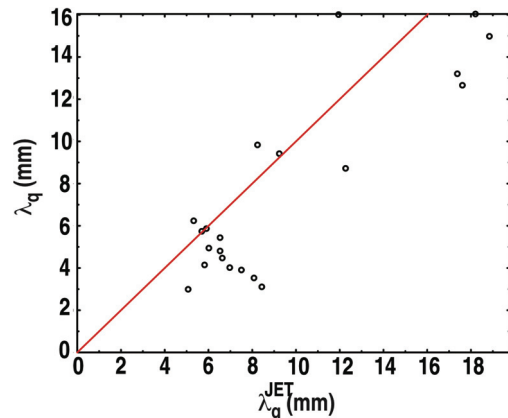


Fig. 5. Plot of $\lambda_q^{\text{DIII-D}}$ vs λ_q^{JET} showing that the DIII-D data fits the JET scaling relation.

widths a factor of 10 lower than the measurements. In addition, there is no size dependence and there is no manifest dependence on I_p .

V. UEDGE Simulations

Efforts are underway to model four representative points on the I_p scan of Fig. 3 with UEDGE [2] in order to determine what underlying physics might be changing with I_p to affect λ_q . Inputs to UEDGE are the power flux through the SOL and the midplane profiles of n_e and T_e . Transport coefficients are adjusted within UEDGE to obtain a match between the experimental and predicted profiles. Results are preliminary but still offer some insight.

Figure 6 shows a comparison of the measured heat flux profile and those obtained from a UEDGE simulation as a function of distance along the target plate for $I_p = 1.5$ MA. With impurities and drifts turned off and with impurities on and drifts off, the predicted profiles are narrow; approximately 50% of the width of the measured profile. Only with the flows (partially) turned on does the profile broaden by producing a shoulder on the SOL side. The profiles on the private flux side are very narrow and nearly constant for the varying conditions. The asymmetry between the private flux region and SOL is also reproduced by the simulation. The results appear to indicate that the plate physics and flows are important in determining the heat flux profile.

This work was supported by the U.S. Department of Energy under DE-AC52-07NA27344, DE-FC02-04ER54698, DE-FG02-07ER54917, and DE-AC04-94AL85000.

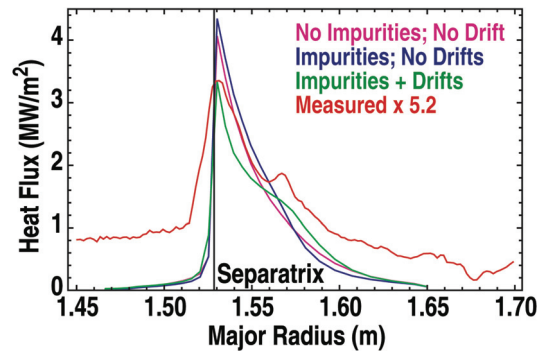


Fig. 6. Heat flux profiles from UEDGE compared with measurement. Impurities have little effect on the profile whereas the flows have a pronounced effect.

- [1] C.S. Pitcher and P.C. Stangeby, *Plasma Phys. Control. Fusion* **39** (1997) 779.
- [2] T. Rognlien, *et al.*, *J. Nucl. Mater.* **196-198** (1992) 347-351.
- [3] G. Kirnev, *et al.*, *Plasma Phys. Control. Fusion* **49** (2007) 689.
- [4] A. Hermann, *et al.*, *Plasma Phys. Control. Fusion* **37** (1995) 17.
- [5] A. Loarte, *et al.*, *J. Nucl. Mater.* **266-269** (1999) 587-592.